Chapter 3

The Schwarzschild Metric and Classical Tests of GR

In this chapter we apply the Schwarzschild metric to describe the spacetime exterior to a star. This will allow us to investigate four **Classical Tests of General Relativity**. These are:-

1. The advance of pericentre of planetary and stellar orbits
2. Gravitational light deflection
3. Gravitational redshift
4. Gravitational time delay

Before we consider each of these tests in turn, we first determine the equations of geodesics for the Schwarzschild metric.

3.1 Geodesics for the Schwarzschild metric

The geodesics for a material 'test' particle in the Schwarzschild metric satisfy equation (2.13), with the proper time, τ, as affine parameter:

$$\frac{d}{dp}\left(g_{\lambda\nu}\frac{dx^\nu}{dp}\right) - \frac{1}{2}\frac{\partial g_{\mu\nu}}{\partial x^\lambda}\frac{dx^\mu}{dp}\frac{dx^\nu}{dp} = 0 \tag{3.1}$$

Notice that the metric coefficients of equation (2.46) are independent of both t and ϕ; hence if we set $\lambda = 0$ and $\lambda = 3$ then the second term on the left hand side of equation (3.1) vanishes. Given also that the Schwarzschild metric is *orthogonal*, it follows that

$$\frac{d}{d\tau}\left(g_{tt}\frac{dt}{d\tau}\right) = \frac{d}{d\tau}\left(g_{\phi\phi}\frac{d\phi}{d\tau}\right) = 0 \tag{3.2}$$

Integrating this gives us

$$g_{tt}\frac{dt}{d\tau} = \text{ constant} \tag{3.3}$$

and

$$g_{\phi\phi}\frac{d\phi}{d\tau} = \text{ constant} \tag{3.4}$$

The geodesic equation for θ (i.e. $\lambda = 2$) follows from equation (2.14):

$$\frac{d}{d\tau}\left(r^2\frac{d\theta}{d\tau}\right) - \frac{1}{2}\frac{\partial}{\partial\theta}\left(r^2\sin^2\theta\right)\left[\frac{d\phi}{d\tau}\right]^2 = 0 \tag{3.5}$$

which reduces to

$$r^2\frac{d^2\theta}{d\tau^2} + 2r\frac{dr}{d\tau}\frac{d\theta}{d\tau} - r^2\sin\theta\cos\theta\left(\frac{d\phi}{d\tau}\right)^2 = 0 \tag{3.6}$$

Equation (3.6) has a particular solution $\theta = \pi/2$; adopting this solution is equivalent to choosing the plane of the orbit of our material particle (e.g. a planet) to lie in the equatorial plane of our coordinate system. Thus

$$\frac{d\theta}{d\tau} = 0 \tag{3.7}$$

Making use of $\theta = \pi/2$ in simplifying equations (3.3) and (3.4), it follows that

$$\frac{dt}{d\tau} = \frac{k}{1 - \frac{2M}{r}} \tag{3.8}$$

and

$$\frac{d\phi}{d\tau} = \frac{h}{r^2} \tag{3.9}$$

where h and k are constants.

We can now use equations (3.8), (3.9) and (3.7) to obtain the geodesic differential equation for r, not directly from equation (2.14) but from equation (1.28)

$$-1 = g_{tt}\left(\frac{dt}{d\tau}\right)^2 + g_{rr}\left(\frac{dr}{d\tau}\right)^2 + g_{\phi\phi}\left(\frac{d\phi}{d\tau}\right)^2 \tag{3.10}$$

which in turn reduces to

$$\left(\frac{dr}{d\tau}\right)^2 = k^2 - 1 - \frac{h^2}{r^2} + \frac{2M}{r}\left(1 + \frac{h^2}{r^2}\right) \tag{3.11}$$

3.2 Planetary orbits in Newtonian theory

The Newtonian equations of motion for a test mass orbiting a mass M (where the orbital plane is taken to be the equatorial plane $\theta = \pi/2$) take the form

$$r^2\frac{d\phi}{dt} = h \tag{3.12}$$

and

$$\frac{d^2r}{dt^2} = -\frac{M}{r^2} + r\left(\frac{d\phi}{dt}\right)^2 \tag{3.13}$$

Note that equations (3.9) and (3.12) are equivalent, apart from the use of proper time, τ, and coordinate time, t, respectively; in Newtonian dynamics, however, there is no distinction between τ and t.

It is customary to solve equation (3.12) by first changing the dependent variable from r to $u = 1/r$, and the independent variable from t to ϕ. Note that

$$\frac{d\phi}{dt} = hu^2 \tag{3.14}$$

and so

$$\frac{dr}{dt} = \frac{d}{dt}\left(\frac{1}{u}\right) = -\frac{1}{u^2}\frac{du}{d\phi}\frac{d\phi}{dt} = -h\frac{du}{d\phi} \tag{3.15}$$

Re-expressing equation (3.13) in terms of u and ϕ gives

$$\frac{d^2u}{d\phi^2} = -u + \frac{M}{h^2} \tag{3.16}$$

This equation has solution

$$u = \frac{M}{h^2}\left(1 + e\cos\phi\right) \tag{3.17}$$

which represents an ellipse, with eccentricity e, semi-major axis a and focus at $r = 0$. The constant h is related to the **semi-latus rectum**, ℓ of the ellipse, viz:-

$$\ell = \frac{h^2}{M} = a(1 - e^2) \tag{3.18}$$

3.3 The advance of pericentre in GR

We can manipulate equation (3.11) in a similar manner to the solution of the Newtonian differential equation (3.15), by changing the dependent variable from r to u and the independent variable from τ to ϕ. Substituting into equation (3.11) this gives

$$h^2\left(\frac{du}{d\phi}\right)^2 = \left(k^2 - 1\right) - h^2u^2 + 2Mu\left(1 + h^2u^2\right) \tag{3.19}$$

Differentiating this equation and cancelling the common factor of $\mathrm{d}u/\mathrm{d}\phi$ gives the result

$$\frac{d^2u}{d\phi^2} = -u + \frac{M}{h^2} + 3Mu^2 \tag{3.20}$$

Comparing equations (3.16) and (3.20) we see that the effect of a GR treatment is to add the extra term $3Mu^2$ on the right hand side. We will now determine the impact of this extra term on the orbital path of a planet moving around a star of mass, M. For typical planetary orbits in the Solar System this extra term is tiny compared with the second term on the right hand side of equation (3.20); e.g. for the Earth's orbit the ratio

$$\frac{3Mu^2}{M/h^2} \simeq 3 \times 10^{-8} \tag{3.21}$$

Hence, because the extra GR term is very small anyway, we can obtain a very good approximation to equation (3.20) by replacing u in the u^2 term on the right hand side by the solution to the *Newtonian* version of this equation, as given by equation (3.17). Thus,we obtain

$$\frac{d^2u}{d\phi^2} = -u + \frac{M}{h^2} + 3\frac{M^3}{h^4}\left(1 + 2e\cos\phi + e^2\cos^2\phi\right) \tag{3.22}$$

We can write u as the sum of a 'Newtonian' and 'GR' part, i.e.

$$u = u_{\rm N} + u_{\rm GR} \tag{3.23}$$

so that $u_{\rm GR}$ describes the correction to the Newtonian orbit. Subtracting off the Newtonian solution, equation (3.22) becomes

$$\frac{d^2u_{\rm GR}}{d\phi^2} = -u_{\rm GR} + 3\frac{M^3}{h^4}\left(1 + 2e\cos\phi + e^2\cos^2\phi\right) \tag{3.24}$$

Noting that

$$\cos^2\phi = \frac{1}{2}\left(1 + \cos 2\phi\right) \tag{3.25}$$

we can rewrite equation (3.24) as

$$\frac{d^2u_{\rm GR}}{d\phi^2} + u_{\rm GR} = 3\frac{M^3}{h^4}\left(1 + \frac{e^2}{2} + 2e\cos\phi + \frac{e^2}{2}\cos 2\phi\right) \tag{3.26}$$

The right hand side of equation (3.26) takes the form

$$A + B\cos\phi + C\cos 2\phi \tag{3.27}$$

where A, B and C are constants. It is easy to verify that particular integrals for each of these terms are, respectively

$$u_{\rm GR} = A \tag{3.28}$$

$$u_{\rm GR} = \frac{1}{2}B\phi\sin\phi \tag{3.29}$$

$$u_{\rm GR} = -\frac{1}{3}C\cos 2\phi \tag{3.30}$$

and the correction to the Newtonian orbit is given by the sum of these three particular integrals. Since each of the constants, A, B and C is of order the tiny constant M^3/h^4, we see that the first and third terms – given by equations (3.28) and (3.30) – add to the Newtonian solution respectively a completely negligible constant and an equally negligible constant plus a tiny "wiggle".

The second term, on the other hand, is of a different form. Although the constant, B, is negligibly small, the presence of the ϕ in equation (3.29) means that this term produces a continually increasing – and thus ultimately non-negligible – effect. From equations (3.17), (3.23), (3.26) and (3.29) we can obtain

$$u = \frac{M}{h^2}\left(1 + e\cos\phi + \frac{3M^2}{h^2}e\phi\sin\phi\right) \tag{3.31}$$

Now given that $3M^2/h^2$ is very small, and then using the approximations $\cos\beta \simeq 1$ and $\sin\beta \simeq \beta$ for small angle β, and the addition formula

$$\cos(\alpha - \beta) = \cos\alpha\cos\beta + \sin\alpha\sin\beta \tag{3.32}$$

we can re-cast equation (3.31) as

$$u = \frac{M}{h^2}\left[1 + e\cos\left(1 - \frac{3M^2}{h^2}\right)\phi\right] \tag{3.33}$$

Comparing equation (3.33) with its Newtonian analogue, equation (3.17), we see that again the solution is elliptical in form and that u (and hence r) is a periodic function of ϕ. Notice, however, that the period, P, is given by

$$P = \frac{2\pi}{1 - 3M^2/h^2} > 2\pi \tag{3.34}$$

This means that the values of r trace out an approximate ellipse, but do not begin to repeat until *after* the radius vector has made a complete revolution. In other words the orbit can be regarded as an ellipse that 'precesses' – as shown in Figure 1, so that the pericentre line advances each orbit by an amount, Δ, given by

$$\Delta = 2\pi\left(1 - \frac{3M^2}{h^2}\right)^{-1} - 2\pi \simeq \frac{6\pi M^2}{h^2} = \frac{6\pi M}{a(1-e^2)} \tag{3.35}$$

If we apply equation (3.35) to the orbit of Mercury, we obtain a perihelion advance which builds up to about 43 seconds of arc per century (see Example Sheet II-1).

3.3.1 GR's first major success

It had been realised since the mid-19th century – when the existence of the planet Neptune was predicted by Adams and Le Verrier from studying its perturbing effect on the orbit of Uranus – that there was something wrong with the Newtonian predictions for the orbit of Mercury. Le Verrier, applying Newtonian perturbation theory, predicted the existence of another planet inside that of Mercury and even gave it a name – Vulcan. He calculated the orbit which Vulcan was required to have, in order to explain the discrepancy between Mercury's observed orbit and the predictions of Newtonian

gravity – after accounting for the perturbing effects of all of the known planets. All attempts to observe Vulcan, however, met with failure.

Einstein's publication of General Relativity in 1916 provided the answer to the mystery of Mercury's orbit. The GR prediction of a perihelion advance matched extremely well the observed discrepancy in Mercury's orbit, and represented the first major success of the theory over Newtonian gravity.

3.3.2 The Binary Pulsar

A much clearer example of pericentre advance can be seen in the **binary pulsar** system PSR 1913+16, discovered in 1974. The orbital period of the system is $P = 0.323$ days, and the periastron is advancing at the rate of more than 4° per year. It is very likely that both members of the binary system are neutron stars. This system has proved to be an excellent laboratory for testing predictions of general relativity and we will consider it again later in this chapter, and in discussing gravitational radiation in Chapter 5.

3.3.3 OJ 287

An even more dramatic example of pericentre advance is the BL Lac object (see Galaxies II course) **OJ 287**, which was discovered in 1891 and is now known to lie at a distance of about 3 billion light years. OJ 287 is believed to comprise a pair of supermassive black holes (see also Chapter 6) the smaller of which has a mass of roughly 10^8 solar masses while the larger – with a mass of about 18 billion solar masses – is thought to be the most massive black hole discovered to date. The smaller black hole

orbits its massive companion with a period of about 12 years, but the orbit appears to precess by more than 30 degrees every orbital period. The orbital semimajor axis is also believed to be shrinking in a manner consistent with the GR prediction that the system is losing energy through gravitational radiation.

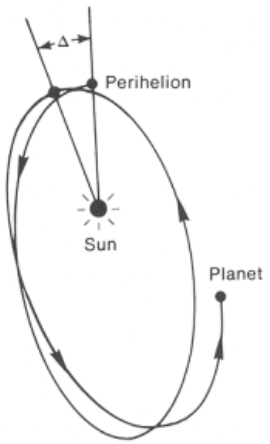

Figure 1

Advance of perihelion, as predicted by General Relativity, resulting in a planetary orbit which is not a closed ellipse, but which precesses slowly.

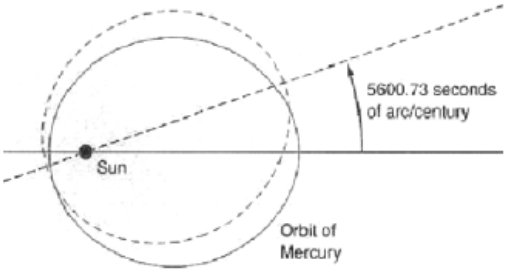

Figure 2

Advance of perihelion of the planet Mercury. All but 43 arcseconds per century of the observed advance of perihelion could be explained simply by Newtonian perturbations by the other known planets; GR provided an explanation for the remaining 43 arcseconds discrepancy. This additional advance is due to the effect of the curvature of spacetime in the vicinity of the Sun: loosely, one can think of this curvature as an additional source of mass-energy which adds to the perturbation on the planet.

3.4 Gravitational light deflection

The second classical test of General Relativity was the deflection of a light ray passing close to a massive object. In GRG-I (and indeed in A2 Relativity) we showed, by considering a lift in free fall, that light deflection is implied by the Strong Principle of Equivalence. In this chapter we examine the effect more formally, within the framework of the Schwarzschild metric.

This classical test attracted much attention in the years immediately following the publication of General Relativity because it was able to be carried out experimentally, by measuring the apparent shift in angular position of stars very close to the limb of the Sun during a total solar eclipse. In 1919 the British astronomer Arthur Eddington led an expedition to the Southern Hemisphere to carry out this test.

It is sometimes written than General Relativity predicts gravitational light deflection while Newtonian gravitation does not. This is only partly true, however. If we regard photons (as, indeed, modern physics holds true) as particles with zero rest mass, then formally they are 'immune' to Newton's gravitational force. If, on the other hand, we regard photons as having a negligible but non-zero mass then – even within a purely Newtonian framework – we can calculate the predicted deflection angle as light passes close to a massive object. In fact, this calculation was first carried out in 1801 by Söldner. Before considering the General Relativistic calculation, it is instructive to derive this Newtonian deflection angle result.

3.4.1 Newtonian light deflection

We consider the path of a photon passing close to a mass, M. In Newtonian dynamics the orbit of the photon during the encounter is a hyperbola, with M at one focus, given by

$$r(\phi) = \frac{r_{\min}(e+1)}{1+e\cos\phi} \tag{3.36}$$

where $e > 1$ is the eccentricity and $r_{\min}$ is the distance of the photon from M at its point of closest approach. This trajectory is shown in Figure 3. The asymptotic directions of the photon before and after the deflecting encounter are given by

$$\phi = \pm\left(\frac{\pi}{2} + \frac{\Delta\phi}{2}\right) \tag{3.37}$$

where $\Delta\phi$ is the total deflection angle (compared with the undeflected trajectory, from $\phi = -\pi/2$ to $\phi = \pi/2$).

As for a planetary elliptical orbit, the motion of the Newtonian photon satisfies

$$r^2\frac{d\phi}{dt} = h \tag{3.38}$$

where h is a constant, related to the semi-latus rectum, ℓ, of the hyperbola via:

$$h^2 \;=\; M\ell \;=\; Ma(e^2-1) \;=\; M\,r_{\min}(e+1) \tag{3.39}$$

The photon also satisfies an **energy equation**

$$\frac{1}{2}v^2 - \frac{M}{r} = \frac{1}{2}\left[\left(\frac{dr}{dt}\right)^2 + r^2\left(\frac{d\phi}{dt}\right)^2\right] - \frac{M}{r} = E_{\text{tot}} \tag{3.40}$$

where the constant E_{tot} is the total energy, equal to the sum of the kinetic and potential energy (remembering that $G = 1$), per unit mass. In equation (3.40) the two terms in the square brackets are, respectively, the squared radial and transverse velocity components.

Writing

$$\frac{dr}{dt} = \frac{dr}{d\phi}\frac{d\phi}{dt} \tag{3.41}$$

and substituting from equation (3.38) it follows that

$$\frac{h^2}{2r^2}\left[\frac{(dr/d\phi)^2}{r^2} + 1\right] - \frac{M}{r} = E_{\text{tot}} \tag{3.42}$$

From equation (3.36)

$$\frac{dr}{d\phi} = \frac{r_{\min}(e+1)e\sin\phi}{(1+e\cos\phi)^2} = \frac{r^2 e\sin\phi}{r_{\min}(e+1)} \tag{3.43}$$

Substituting into equation (3.42), and after a little algebra we obtain

$$E_{\text{tot}} = \frac{M(e-1)}{2r_{\min}} \tag{3.44}$$

From equation (3.36) we see that $r \to \infty$ when $\cos\phi = -1/e$. Also, setting $v = c = 1$ for $r \to \infty$, from equation (3.40) we see that

$$E_{\text{tot}} = \frac{1}{2} \tag{3.45}$$

Rearranging equation (3.44) it follows that, since $e >> 1$

$$e = 1 + \frac{r_{\min}}{M} \simeq \frac{r_{\min}}{M} \tag{3.46}$$

Hence the asymptotic direction of the outgoing photon is

$$\cos\phi = \cos\left(\frac{\pi}{2} + \frac{\Delta\phi}{2}\right) = -\sin\left(\frac{\Delta\phi}{2}\right) = -\frac{M}{r_{\min}} \tag{3.47}$$

Since $\Delta\phi << 1$,

$$\Delta\phi = \frac{2M}{r_{\min}} \tag{3.48}$$

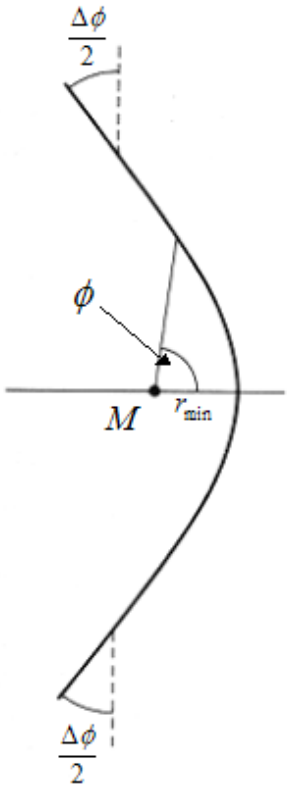

Figure 3

Trajectory of a deflected light ray passing close to a mass, M

The total deflection angle is seen to be twice the angle between the asymptote of the trajectory and the dashed line (the undeflected trajectory)

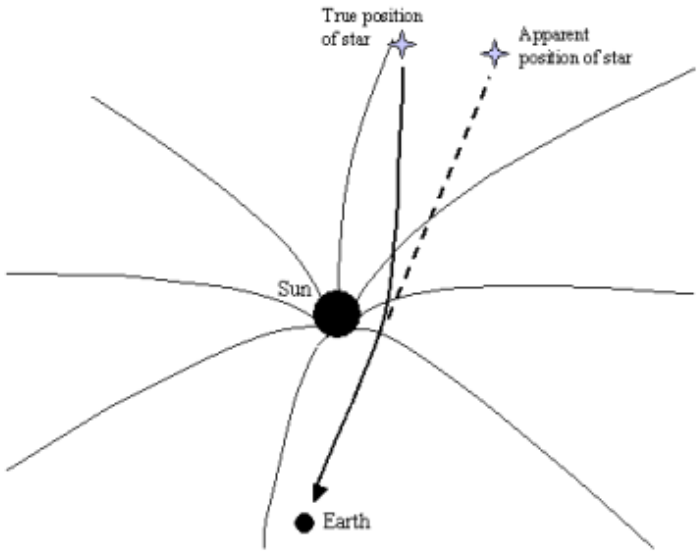

Figure 4

Schematic diagram showing the deflection of a light ray from a background star as it passes close to the Sun. This gravitational light deflection can be observed during a total solar eclipse, and is also seen in radio observations of distant quasars when they lie close to the Sun on the sky.

3.4.2 Light deflection in General Relativity

The geodesics for a photon in the Schwarzschild metric may be derived in a similar manner to Section 3.1, but we now must introduce a new affine parameter, λ (say), since the proper time for a photon is zero.[1]

For the 't' and 'ϕ' geodesic equations it is straightforward to see that we again obtain equations of the form

$$\frac{dt}{d\lambda} = \frac{k}{1-2M/r} \tag{3.49}$$

$$\frac{d\phi}{d\lambda} = \frac{h}{r^2} \tag{3.50}$$

since, for the 'θ' equation, we can again spot the particular solution $\theta = \pi/2$. It obviously then also follows that

$$\frac{d\theta}{d\lambda} = 0 \tag{3.51}$$

We can then use equation (1.30) to obtain

$$\left(\frac{dr}{d\lambda}\right)^2 = k^2 - \frac{h^2}{r^2} + \frac{2Mh^2}{r^3} \tag{3.52}$$

We now proceed as in Section 3.3, replacing the dependent variable, r by $u = 1/r$, and the independent variable λ by ϕ. This gives us

$$\frac{d^2u}{d\phi^2} + u = 3Mu^2 \tag{3.53}$$

If we ignore the term on the right hand side we can see that a particular integral is

$$u = \frac{\cos\phi}{r_{\min}} \tag{3.54}$$

Following the same approach as Section 3.3, we can obtain a very good approximation to equation (3.53) by replacing u on the right hand side by equation (3.54). This gives

[1] In fact, the choice of affine parameter will not be important, since we will determine the trajectory of the photon with the coordinate ϕ as the independent variable

the equation

$$\frac{d^2u}{d\phi^2} + u = \frac{3M}{r_{\min}^2}\cos^2\phi = \frac{3M}{2r_{\min}^2}\left(1 + \cos 2\phi\right) \tag{3.55}$$

It is straightforward to verify that a particular integral of this approximation is

$$u = \frac{3M}{2r_{\min}^2}\left(1 - \frac{1}{3}\cos 2\phi\right) \tag{3.56}$$

from which it follows that the general solution of equation (3.53) is

$$u = \frac{\cos\phi}{r_{\min}} + \frac{3M}{2r_{\min}^2}\left(1 - \frac{1}{3}\cos 2\phi\right) \tag{3.57}$$

Using equation (3.37) we can rewrite this, for e.g. the outgoing photon trajectory, as

$$u = \frac{\cos\left(\frac{\pi}{2} + \frac{\Delta\phi}{2}\right)}{r_{\min}} + \frac{3M}{2r_{\min}^2}\left[1 - \frac{1}{3}\cos\left(\pi + \Delta\phi\right)\right] \tag{3.58}$$

or

$$u = -\frac{\sin(\Delta\phi/2)}{r_{\min}} + \frac{3M}{2r_{\min}^2}\left[1 + \frac{1}{3}\cos\Delta\phi\right] \tag{3.59}$$

which further simplifies, since $\Delta\phi << 1$, to

$$u = -\frac{\Delta\phi}{2r_{\min}} + \frac{2M}{r_{\min}^2} \tag{3.60}$$

Setting $u = 0$ (i.e. $r \to \infty$) this finally gives us the General Relativistic result

$$\Delta\phi = \frac{4M}{r_{\min}} \equiv \frac{4GM}{c^2 r_{\min}} = \frac{2R_{\rm S}}{r_{\min}} \tag{3.61}$$

This is exactly twice the deflection angle predicted by our earlier Newtonian treatment. If we take $r_{\min}$ to be the radius of the Sun (which would correspond to a light ray grazing the limb of the Sun from a background star observed during a total solar eclipse – see Figure 4) then we find that

$$\Delta\phi = \frac{4 \times 1.5 \times 10^3}{6.95 \times 10^8} = 8.62 \times 10^{-6} \text{ radians} \quad = \quad 1.77 \text{ arcsec} \tag{3.62}$$

The validity of the General Relativity result for the gravitational deflection of light was supported by the observations made by the Eddington expedition, and more recently

has been repeatedly verified with much greater precision by radio observations of distant quasars when they are closely aligned with the solar limb.

The General Relativity light deflection formula also lies at the heart of the field of gravitational lensing – one of the most active areas of research in astronomy and cosmology today.

3.4.3 Gravitational lensing

Figure 5 shows the path of a light ray from a distant source deflected through an angle, α, by a close encounter with a point mass, M, which is exactly collinear with the source and observer. Since the deflection angle is small (in Figure 5 it is, of course, greatly exaggerated) we can represent the deflection as taking place at a single point, P, a perpendicular distance R_E from M, as shown. The photon path can then be approximated by the lines OP and PS.

By symmetry the point P must lie on circle of radius R_E in the plane perpendicular to OS, such that *any* point on the circle represents a possible point of deflection. Thus, the point mass, M, essentially acts as a **gravitational lens**, focussing light rays from the source at the observer, who will see an image of the source as a *ring*, or radius R_E.

This circle is shown schematically in the lower panel of Figure 5. It is known as an **Einstein Ring** and R_E is referred to as the **Einstein Radius** of the gravitational lens (although it was not Einstein but Chwolson, in 1924, who first predicted theoretically the existence of this ring).

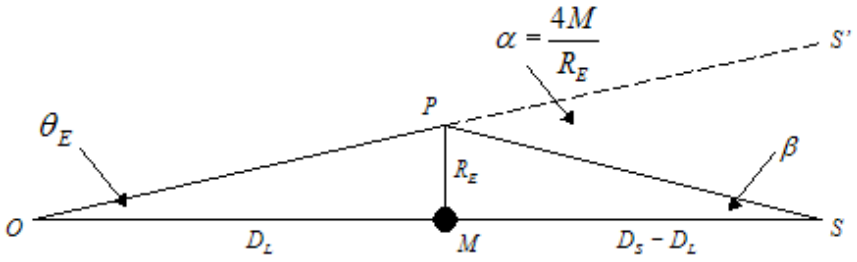

Figure 5

Gravitational deflection of light rays from a source at distance D_S, through an angle, α, by a point mass, M, at distance D_L from the observer, O. The source, deflecting mass and observer are assumed to be exactly collinear. For small deflection angle, α, we may regard the deflection as taking place at a single point, P, a distance R_E from M. The deflecting mass acts as a gravitational lens, producing an image of the source which is an **Einstein Ring** of angular radius θ_E, as shown below (from Mollerach & Roulet 2002)

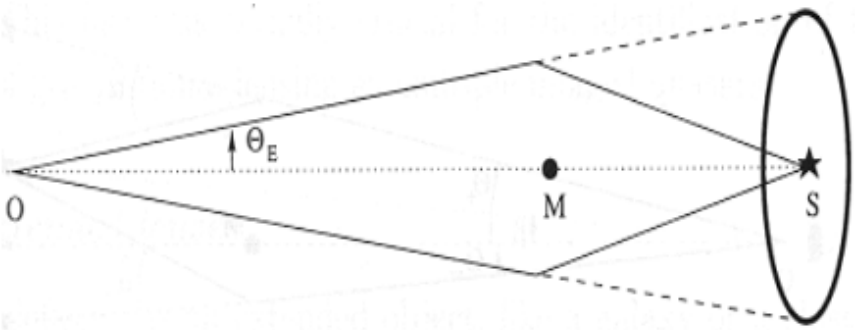

We can determine the angular radius, θ_E of the Einstein Ring as follows. Let D_L and D_S denote the distance of the gravitational lens and source respectively. From Figure 5 it is easy to see that

$$\theta_E + \beta = \alpha \tag{3.63}$$

Also,

$$\theta_E = \frac{R_E}{D_L} \tag{3.64}$$

and

$$\beta \;=\; \frac{R_E}{D_S - D_L} \;=\; \theta_E \frac{D_L}{D_S - D_L} \tag{3.65}$$

Substituting for β and α in equation (3.63) gives

$$\theta_E \;+\; \theta_E \frac{D_L}{D_S - D_L} \;=\; \theta_E \frac{D_S}{D_S - D_L} \;=\; \frac{4M}{R_E} \;=\; \frac{4M}{D_L \theta_E} \tag{3.66}$$

i.e.

$$\theta_E = \sqrt{\frac{4M(D_S - D_L)}{D_S D_L}} \tag{3.67}$$

Writing $x = D_L/D_S$ we can rewrite equation (3.67) as

$$\theta_E = \sqrt{\frac{4M(1-x)}{D_S\, x}} \tag{3.68}$$

Einstein Rings are also expected when the gravitational lens is an extended mass distribution which is spherically symmetric and is exactly aligned with the source and the observer; in this case M in equation (3.68) is the total mass inside the projected angular radius, θ_E. When the lensing mass is off-axis, and / or is not spherically symmetric then instead of an Einstein ring multiple images of the source are produced, the angular separation of which is of order θ_E.

Suppose, for example, a foreground galaxy lenses a background quasar or galaxy. It is straightforward to verify that equation (3.68) is conveniently expressed in this case as

$$\theta_E \simeq 3\text{”} \sqrt{\frac{M}{10^{12} M_\odot} \frac{10^9\,\mathrm{pc}}{D_S} \frac{(1-x)}{x}} \tag{3.69}$$

and consequently typical image separations are of order a few arcseconds, and should be resolvable separately. This regime is known as **strong gravitational lensing**.

In the past few decades hundreds of examples of strong lensing have been observed

– mainly at radio and optical wavelengths – and the magnification and shape of the source images can be used to constrain the mass of the lens.

Consider now the case of lensing by stars within the Milky Way galaxy. In this case the angular Einstein Radius is conveniently expressed as

$$\theta_E \simeq 0.9\,\mathrm{mas}\sqrt{\frac{M}{M_\odot}\frac{10\,\mathrm{kpc}}{D_S}\frac{(1-x)}{x}} \tag{3.70}$$

(where 'mas' denotes milliarcseconds). Hence, the images in this case are (currently) too close together to be resolved. This regime is known as **gravitational microlensing**.

Although the microlensed images cannot be resolved, they do, however, change the apparent brightness of the source star. Moreover, if the lens is moving across the line of sight we can detect the change in magnification of the source as the projected lens-source angular separation changes.

Since the early 1990s a number of monitoring programs have been observing crowded stellar fields in the Galactic Bulge and the Magellanic Clouds, searching for the signatures of microlensing from intervening MACHOs (MAssive Compact Halo Objects). Several hundred microlensing events have been detected to date, and analysis of their **light curves** (i.e. how the apparent brightness of the sources changes with time) has allowed the mass of the lensing MACHOs to be constrained – results which have had important implications for cosmological searches for dark matter.

3.5 Gravitational redshift of light

In GRG-I and A2 Relativity we used the Strong Principle of Equivalence to show that a photon 'climbing out' of a gravitational field is seen to be redshifted when it arrives at a distant observer. We now derive the same result within the framework of the Schwarzschild metric.

Suppose that light emitted at the event with coordinates (t_e, r_e) in the Schwarzschild metric travels along a radial null geodesic (i.e. with $d\theta = d\phi = 0$) to reach a distant observer at the event with coordinates (t_o, r_o). From equation (2.46)

$$ds^2 = 0 = -\left(1 - \frac{2M}{r}\right) dt^2 + \frac{dr^2}{1 - 2M/r} \tag{3.71}$$

i.e.

$$\int_{t_e}^{t_o} dt = t_o - t_e = \int_{r_e}^{r_o} \frac{dr}{1 - 2M/r} \tag{3.72}$$

Suppose we now think of the light as a wave, of frequency ν_e as measured in its rest frame. Suppose two adjacent wavecrests leave r_e at coordinate time t_e and $t_e + \Delta t_e$, and reach r_o at coordinate time t_o and $t_o + \Delta t_e$. Between the two emission events the elapsed proper time, $\Delta\tau_e$ is given by

$$\Delta\tau_e = \Delta t_e \sqrt{1 - \frac{2M}{r_e}} \equiv \frac{1}{\nu_e} \equiv \lambda_e \tag{3.73}$$

(recalling that $c = 1$).

For the observer at (t_o, r_o) the elapsed proper time between the arrival of the two wavecrests is

$$\Delta\tau_o = \Delta t_e \sqrt{1 - \frac{2M}{r_o}} \equiv \frac{1}{\nu_o} \equiv \lambda_o \tag{3.74}$$

Hence, the gravitational redshift of the light is given by

$$z \equiv \frac{\lambda_o - \lambda_e}{\lambda_e} = \sqrt{\frac{1 - 2M/r_o}{1 - 2M/r_e}} - 1 = \sqrt{\frac{r_e(r_o - R_S)}{r_o(r_e - R_S)}} - 1 \tag{3.75}$$

where R_S is the Schwarzschild radius of the central mass, M.

Consider light emitted from the Solar photosphere, at $r_e = R_\odot$, and observed at the distance of the Earth. Since $r_o >> r_e >> R_S$ (and ignoring the *blueshift* of the light as it falls into the gravity field of the Earth), equation (3.74) simplifies to

$$z \simeq \left(1 - \frac{M}{r_o}\right)\left(1 + \frac{M}{r_e}\right) - 1 \simeq \frac{M}{r_e} \tag{3.76}$$

Thus, the gravitational redshift of e.g. spectral line emitted at the Solar photosphere is

$$z = \frac{1.5 \times 10^3}{6.95 \times 10^8} \simeq 2 \times 10^{-6} \tag{3.77}$$

This effect is too small to be observed, since it is dwarfed in magnitude by the various astrophysical processes which contribute to the broadening of spectral lines (e.g. thermal, natural and collisional broadening). It has been successfully measured, however, in the spectra of **white dwarf stars**. These compact evolved stars have masses comparable to that of the Sun, but radii comparable to that of the Earth. Hence, one finds that

$$z = \frac{1.5 \times 10^3}{6.4 \times 10^6} \simeq 2.3 \times 10^{-4} \tag{3.78}$$

which is measurable (but only just!).

Perhaps the most convincing evidence for gravitational redshift comes from a terrestrial experiment, carried out by Pound, Rebka and Snider in 1960, using very high frequency gamma rays emitted at the foot and observed at the top of a 22m high tower at Harvard

University. Although the predicted redshift was only about 2×10^{-15} in this case, it could be measured because the frequency of the gamma rays was known to extremely high precision, due to a resonance known as the **Mossbauer effect**. (See Green Schutz, page 120 for more details).

3.6 Gravitational time delay

The fourth classical test of General Relativity is closely related to the third test: gravitational redshift. In the previous section we saw that two events separated by coordinate time interval dt_e correspond to different intervals of proper time when observed at different radial coordinates, r_e and r_o respectively in the Schwarzschild metric.

In this section we show that, besides experiencing a deflection when passing close to a gravitating mass, light also experiences a time delay compared to the travel time in the absence of the mass.

The time delay has 2 contributions: the first is purely geometric, arising from the fact that the deflected trajectory is longer than the undeflected one. The second delay is gravitational, and is known as the **Shapiro Effect**. It comes about because clocks run more slowly in a gravitational field.

We can obtain a simple expression for the Shapiro Effect as follows. Consider first the invariant interval of the Schwarzschild metric expressed in its usual form

$$ds^2 = -\left(1 - \frac{2M}{r}\right) dt^2 + \frac{dr^2}{\left(1 - \frac{2M}{r}\right)} + r^2 d\theta^2 + r^2 \sin^2\theta d\phi^2 \tag{3.79}$$

Suppose we now introduce a new radial coordinate, R, via the equation

$$r = R\left(1 + \frac{M}{2R}\right)^2 \tag{3.80}$$

(note that R still has dimensions of length). Since we are considering (for the moment at least) the GR effects of a weak gravitational field, such as that of the Sun, we may safely assume that $M << r$ and hence $M << R$. Thus, we may approximate equation (3.80) by

$$r \simeq R\left(1 + \frac{M}{R}\right) \tag{3.81}$$

Noting that

$$1 - \frac{2M}{r} = \frac{r - 2M}{r} \tag{3.82}$$

and substituting for r from equation (3.81), equation (3.79) becomes

$$ds^2 = -\left(\frac{1 - M/R}{1 + M/R}\right) dt^2 + \left(\frac{1 + M/R}{1 - M/R}\right) dr^2 + R^2\left(1 + \frac{M}{R}\right)^2 \left[d\theta^2 + \sin^2\theta d\phi^2\right] \tag{3.83}$$

Using the binomial expansion for $x << 1$,

$$(1 + x)^n \simeq 1 + nx \tag{3.84}$$

and noting that to first order,

$$dr = dR \tag{3.85}$$

equation (3.83) simplifies further to

$$ds^2 = -\left(1 - \frac{2M}{R}\right) dt^2 + \left(1 + \frac{2M}{R}\right)\left[dR^2 + R^2 d\theta^2 + R^2 \sin^2\theta\, d\phi^2\right] \tag{3.86}$$

Defining Cartesian coordinates

$$X = R\sin\theta\cos\phi, \qquad Y = R\sin\theta\sin\phi, \qquad Z = R\cos\theta \tag{3.87}$$

and introducing the **weak field** (i.e. Newtonian) gravitational potential, ψ, given by

$$\psi = -\frac{M}{R} \equiv -\frac{GM}{R} \tag{3.88}$$

equation (3.86) reduces to

$$ds^2 = -(1+2\psi)\,dt^2 + (1-2\psi)\left[dX^2 + dY^2 + dZ^2\right] \tag{3.89}$$

Thus, we have reduced the spatial part of the metric to the Euclidean separation, re-scaled by the Newtonian potential.

Consider now the trajectory of a photon propagating between a source, at A, and an observer, at B, as shown in Figure 6. Since the deflection due to mass, M, is very small, we can approximate the trajectory as a straight line and introduce new coordinates, (x, y, z), such that the z-axis coincides with the photon trajectory. (Note that this means we neglect the geometric time delay). Consequently $dx = dy = 0$, and we may re-write equation (3.89) as

$$ds^2 = -(1+2\psi)\,dt^2 + (1-2\psi)\,dz^2 \tag{3.90}$$

Since $ds^2 = 0$, it follows that, to first order, the elapsed coordinate time between the emission and arrival of the photon is given by

$$dt^2 = \frac{1-2\psi}{1+2\psi}dz^2 \simeq (1-2\psi)^2\,dz^2 \tag{3.91}$$

i.e.

$$\int dt = \int (1-2\psi)\,dz \tag{3.92}$$

Hence,

$$t_{\rm B} - t_{\rm A} = (z_{\rm B} - z_{\rm A}) - 2\int_{z_{\rm A}}^{z_{\rm B}} \psi(z)dz \tag{3.93}$$

The second term is the gravitational time delay:-

$$\delta t_{\rm grav} = -2\int_{z_{\rm A}}^{z_{\rm B}} \psi(z)dz \tag{3.94}$$

or, in more conventional units

$$\delta t_{\rm grav} = -\frac{2}{c^3}\int_{z_{\rm A}}^{z_{\rm B}} \psi(z) dz \tag{3.95}$$

Thus, the gravitational time delay depends on the gravitational potential integrated along the photon's path.

The Shapiro delay has been measured using radar pulses bounced off Venus and Mercury, when those planets are closely aligned with the Sun. The results show impressive agreement with the predictions of General Relativity (see Figure 7).

The time delay is also very clearly seen in the arrival times of radio pulses from the binary pulsar system PSR 1913+16 (see Figure 8). Again the agreement with GR is excellent.

Finally, the Shapiro Effect is seen in the multiple images of gravitationally lensed quasars. It is possible to measure the time delay because quasars show intrinsic variations in their brightness and spectra. When such variations occur they are seen at different times in the different lensed images.

By carefully measuring the time delay between images and modelling the mass distribution of the lensing mass, it is possible to estimate the proper distance to the quasar. One may, then, combine this distance estimate with the observed redshift of the quasar to estimate the Hubble constant. This method has the advantage over more traditional 'Distance Ladder' estimates in that H_0 is measured on truly cosmological scales, where the observed redshift is unaffected by galaxy peculiar velocities.

3.6.1 Beyond the Shapiro effect?

The results derived in the previous section were for the case of a *static* metric. What if the gravitating mass is moving, or rotating, in the observer's frame as light propagates through the spacetime in its vicinity? In this case the Schwarzschild metric results are inapplicable because their assumption of a static central mass breaks down. In recent literature it has been suggested that observations of close binary pulsars may permit the measurement of gravitational time delay for the case where the gravitating mass *is* moving appreciably over the light crossing time of the system.

One exciting possibility is that such observations may permit measurement of the *speed of propagation* of gravitation. In General Relativity the gravitational field – which of course causes the deflection and time delay of a propagating light ray – is not generated instantaneously but propagates at the speed of light. Hence, crudely, one can reason that for a moving central mass, by the time the influence of the gravitational field has reached a material particle or photon in the surrounding spacetime, the mass will have moved to a new position – 'dragging' along with it the gravitational field which it generates.

Another (somewhat loose, but helpful) way of thinking about this is to say that the particle or photon experiences a 'retarded' gravitational field – arising from where the mass *was* a short time (in fact the light travel time, if GR is correct) before, rather than from where the mass has moved to by the time the effects of the gravitational field reach the particle. (A similar retarded phenomenon is seen with the electromagnetic fields generated by moving charges).

In recent literature there have been some claims that this gravitational retardation effect has been measured; these claims remain deeply controversial, but are likely to be a highly active area of theoretical and observational research in the future.

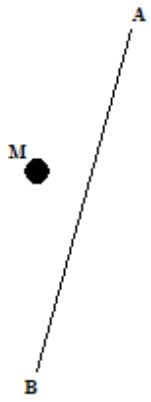

Figure 6

Trajectory of a light ray propagating from a source, A, to an observer, B, passing close to a mass, M

Figure 7

Radar time delay of signals reflected from Venus and passing close to the Sun; comparison of theory with observations. (From Shapiro,1970)

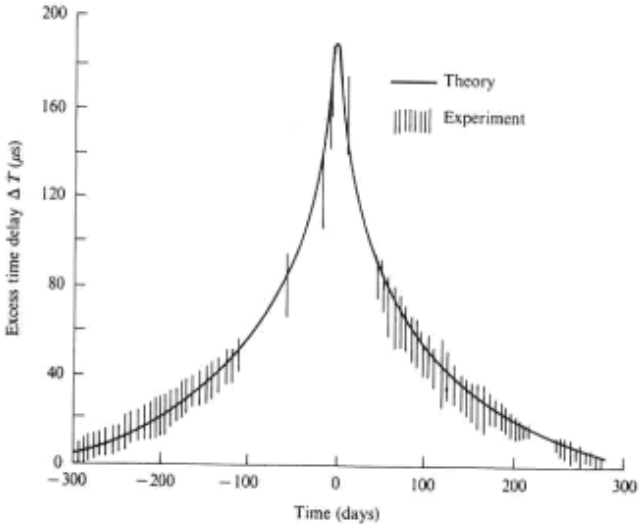

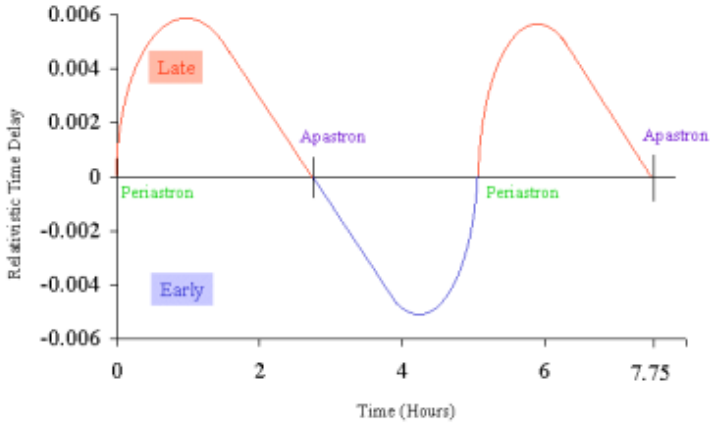

Figure 8

Time delay in the arrival of pulses from the binary pulsar PSR 1913+16. The observed data show excellent agreement with the predictions of GR